EXPERIENCE WITH EMPIRICAL CRITERIA FOR ROTATING STALL IN RADIAL VANELESS DIFFUSERS

by

John W. Fulton

Engineering Associate

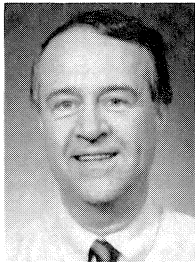Exxon Research and Engineering

Florham Park, New Jersey

and

William G. Blair

Supervisor, Compressor Design

Cooper-Bessemer Rotating Products

Mount Vernon, Ohio

John W. Fulton is an Engineering Associate with Exxon Research and Engineering Company at Florham Park, New Jersey. In his 23 years with Exxon, he has worked in all phases of machinery engineering and in research and development. Mr. Fulton currently chairs the Machinery R&D Network at Exxon. He enjoyed years of assignments in Libya, Venezuela, Alaska, London, and Kuala Lumpur. He has published papers on case histories of vibration problems caused by rotordynamic instability and by rotating stall in high pressure centrifugal compressors. Mr. Fulton is currently Chairman of the Research Advisory Committee of the Pipeline and Compressor Research Council, and a member of their board of directors. He also sits on the Compressor Research Supervisory Committee of the Pipeline Research Committee.

Mr. Fulton has a B.S. degree (Mechanical Engineering) from New Jersey Institute of Technology.

William G. Blair is Supervisor of Compressor Design at Cooper-Bessemer Rotating Products, Mount Vernon, Ohio, a division of Cooper Cameron Corporation. His job responsibilities include oversight of all design and development activities for centrifugal compressors at Cooper. He has been employed at Mount Vernon since graduating from The Pennsylvania State University with an M.S.M.E. degree (1987). Prior to graduate school he received a B.S.M.E. (1986) from Bradley University. Since then, Mr. Blair has added an M.B.A. (1992) from Ashland University, been registered as a Professional Engineer in the State of Ohio, and become a member of ASME.

ABSTRACT

A seven stage, centrifugal compressor, for gas lift service on a North Sea oil production platform, exhibited subsynchronous shaft vibrations during full load, high density, factory tests. Pressure transducers in each stage characterized two stages as stalled and traced the cause of rotor vibration to rotating stall in the diffuser of the last stage. Modifications to that diffuser of the last stage corrected the subsynchronous shaft vibration. The other stage that exhibited characteristics of diffuser rotating stall was left unchanged as it did not yield harmful subsynchronous shaft vibration.

The original compressor configuration was designed to meet Senoo and Kinoshita's criterion [1, 2] for inception of rotating stall in a vaneless diffuser. However, its diffuser widths, b_3, were less than the impeller tip widths, b_2, while b_3 and b_2 widths were equal in Senoo's experiment. Kobayashi, Nishida, et al. [3], and Nishida, et al. [4], extended Senoo's criteria by accounting for a b_3/b_2 ratio less than one. The subject compressor was analyzed using the Kobayashi, et al. [3], criterion. Data reduction of the testing condition producing diffuser rotating stall demonstrated significant margin to the criterion. The generous shape of the inlet diffuser contour was suggested as being the source of the disparity between the criterion and the data reduction values.

EQUIPMENT AND SERVICE

The compressor of this study was the high pressure inboard compressor of a two compressor train. The rated conditions (Table 1) included a specific gravity of 0.92 and rated discharge pressure of 174 Bara (2526 psia). The compressor operated between the first and second lateral critical frequencies of the rotor support system. The design resulted in a first critical (approximately 4000 cpm) 23.6 percent below the compressor minimum continuous speed, while the second critical (approximately 10,000 cpm) had a margin of 27.3 percent above maximum continuous speed. Additional features of this compressor (Figure 1) included dry gas seals and individual stage casing drains.
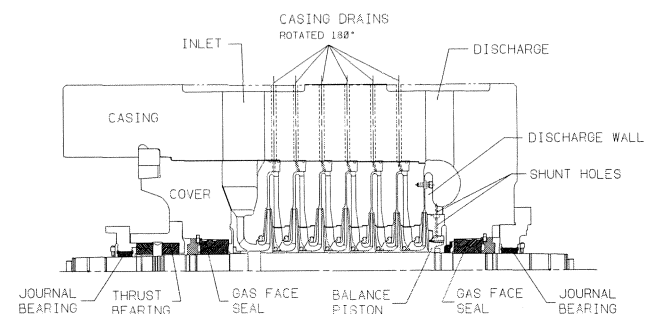

Figure 1. Compressor Schematic.

Table 1. Compressor Rated Conditions.

Q_i – ACMS (ACFM)	0.61	(1301)
P_i – Bara (psia)	40.3	(585)
T_i – °C (°F)	35.7	(96.3)
ρ_i – kg/m³ (lb_m/ft³)	52.8	(3.3)
P_d – Bara (psia)	174.0	(2526)
T_d – °C (°F)	150.7	(303.3)
ρ_d – kg/m³ (lb_m/ft³)	153.3	(9.6)
Gas Type – (MW)	Nat. Gas	(26.6)
N – RPM	7381	

Table 2. Compressor Full Load, High Density, Test Conditions.

Q_i – ACMS (ACFM)	0.66	(1405)
P_i – Bara (psia)	34.5	(500)
T_i – °C (°F)	37.8°	(100°)
ρ_i – kg/m³ (lb_m/ft³)	54.3	(3.4)
P_d – Bara (psia)	169.3	(2456)
T_d – °C (°F)	236.2°	(457.2°)
ρ_d – kg/m³ (lb_m/ft³)	169.3	(10.58)
Gas Type – (MW)	Inert	(37.6)
N – RPM	7381	

BASELINE TESTING

Initial testing of the high pressure compressor occurred at low pressure on the manufacturer's compressor test stand. Mechanical testing followed the guidelines of API Standard 617 Centrifugal Compressors for General Refinery Service [5], and included a four hour test at maximum continuous speed. Aerodynamic performance was measured under Class III conditions following the guidelines of ASME PTC 10-1965 for Compressors and Exhausters [6]. The compressor scope of supply included eddy current type shaft proximity probes that were used in both tests. External instrumentation consisted of diaphragm type, pressure transmitters, and thermocouples for flange pressure and temperature measurement, respectively. The performance test incorporated test loop flow measurement by means of an orifice plate. Neither of these tests produced a substantial subsynchronous rotor vibration component as seen by the proximity probes.

FULL LOAD TESTING

The customer was concerned about rotor stability due to cross-coupling effects. Together, the manufacturer and customer established full load high density test conditions. The test requirements included the use of the contract driver, gear, base, and auxiliary systems. Safety and schedule concerns dictated the use of inert gases during all testing. Despite this constraint, the test conditions achieved flange-flange aerodynamic similarity at rated speed. Additionally, the field discharge density was exceeded. The specifics of the test conditions are listed in Table 2. These test conditions included the compromise of high gas discharge temperatures approaching 243°C (470°F) at rated speed surge flow.

Instrumentation for the full load, high density test included the internal eddy current type shaft proximity probes. External instrumentation consist of diaphragm type pressure transmitters for flange pressure, thermocouples for temperature measurement, and an orifice plate for flow measurement. The compressor proximity probes detected subsynchronous, rotor vibration, while hand held accelerometers confirmed that no bearing housing, casing, base, nor test pipe vibration existed. Additionally, the test crew installed external diaphragm type pressure transmitters to the individual stage casing drains to aid in the diagnoses of the vibration.

FULL LOAD TEST RESULTS

The test occurred under three distinct compressor configurations with the third configuration being successful at eliminating a substantial, subsynchronous, rotor vibration component.

Configuration I

Compressor proximity probes adjacent to the journal bearings measured a 24 Hz subsynchronous rotor vibration of compressor Configuration I. The subsequent investigation of Configuration I eliminated all potential mechanical sources of subsynchronous vibration. The test participants then suspected aerodynamically induced sources as the cause of the rotor vibration [7, 8, 9, 10]. The vibration amplitude behaved as a discrete function of flow and speed (i.e., flow coefficient) and as a continuous function of pressure. Neither mole weight nor suction temperature could be varied during the testing period, therefore, the density could not be varied by any means other than pressure. Several unsuccessful attempts at reaching the test conditions outlined in Table 2, due to the subsynchronous component causing the unfiltered compressor vibration to exceed the vibration protection shutdown limits, led the participants to terminate the testing of Configuration I.

Upon evaluation of the Configuration I test data, the participants concluded that prerequisites for high vibration included both high gas density and an aerodynamic instability. Since the compressor vibration exceeded alarm levels at the rated conditions, elimination of the flow instability was required. Literature indicated that aerodynamically induced vibration frequencies below 20 percent of the running speed were indicative of diffuser induced rotating stall [11]. The 24 Hz response fell just below this threshold that lead to a focus of efforts toward the redesign of the diffusers in the last, three, compressor stages.

During the disassembly of Configuration I, assembly personnel discovered plastic deformation on the last stage diaphragm resulting in an enlargement of the last stage diffuser width. This discovery reenforced the efforts toward a redesign of the last stage diaphragm. In addition, it cast significant doubt over the usefulness of the test data, leading the authors to omit the data herein.

Configuration II

The Configuration II test yielded subsynchronous vibration (Figure 2) similar to that found in the test of Configuration I. The test crew documented the compressor map to the extent that the vibration difficulties allowed. The compressor performance (head *vs* flow) map shown in Figure 3, includes the stall inception and the stall induced vibration alarm level superimposed.

The test of this configuration included diaphragm type pressure transmitters at the high pressure drains offering both compressor performance insight on a stage by stage basis and the ability to monitor the signals for pressure fluctuation. The
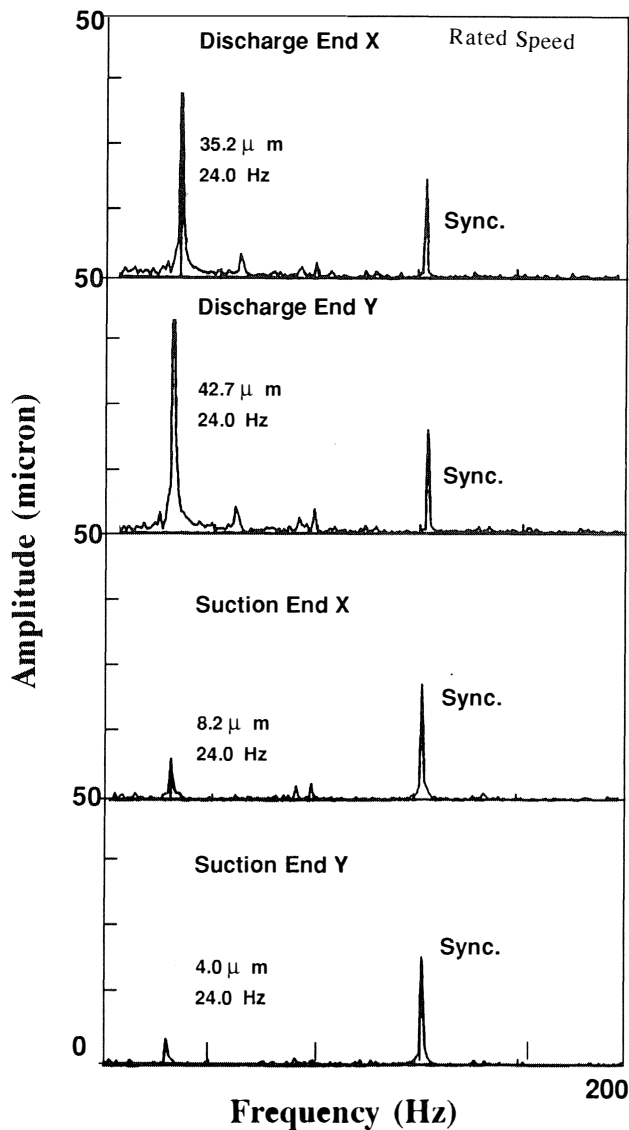
Figure 2. Compressor Vibration Spectra—Configuration II.

Figure 3. Compressor Performance Envelope.

aerodynamic performance evaluation on a stage-to-stage basis and far greater insight. Unfortunately, access was very restricted and the need for expedience in the testing program did not allow the time for a solution.

Based on the experience of the first test the Configuration II test included a capacitance proximity probe in the last stage discharge wall. This probe measured the diffuser width (b_3) at a midradial location in the last stage. The capacitance probe monitored the elastic deformation and thermal growth effects of the last stage diaphragm during testing. The diffuser width grew by 15 percent above nominal under high pressure conditions.

The continued subsynchronous vibration necessitated further changes to the compressor stator. The results of the Configuration II test prompted decisive action by directing the design focus onto the last stage diffuser. The results lent themselves to an extrapolation of the last stage diffuser in order to move the rotating stall inception point to flow levels below the compressor operating envelope.

Configuration III

The seventh stage diffuser was modified in preparation for this testing in three ways: First, struts, installed across the seventh stage diffuser flowpath, were used to attach the discharge wall to the end of the inner casing (Figure 1). The discharge wall was previously mounted to the closed end of the casing. The struts allowed the two sides of the radial diffuser to move together and to maintain a constant diffuser width at any pressure and eliminate the effects of differential thermal expansion. Secondly, shunt holes were added between the discharge plenum and balance seal, as shown in Figure 1. This provided for the supply of the balance seal flow from the plenum through the shunt holes to the seal. Previously, the balance seal flow traveled directly down the back face of the seventh stage impeller, allowing the balance flow to bypass the diffuser altogether. Third, a further reduction in diffuser width was implemented resulting in a pinch of the diffuser to impeller tip width ratio (b_3/b_2) of 0.48.

The rotor vibration and relative pressure fluctuation traces for a test point at rated speed and at a flow slightly greater than incipient surge taken during Configuration III testing are shown in Figures 5 and 6, respectively. No 24 Hz vibration was remaining. An approximate 13.5 Hz, vibration signal emerged in both figures; the source of this vibration was at stage four. The reason for the shift in frequency of the stage four diffuser stall from the 10 Hz found in Configuration II remained unexplored. However, since the vibration level was well within code acceptance limits [5], and due to the low density of the gas at stage four, it was

transmitters (that were the only type available on short notice) were not designed for monitoring pressure fluctuations and significantly attenuated the fluctuating signal. The piping distance between the sensors and the internal fluctuation source compounded the attenuation of the pressure signal. Therefore, absolute levels of pressure fluctuations could not be reliably measured, but the near exact correlation with the shaft vibration frequency as measured by the proximity probes, lead to the conclusion that the frequency of the pressure fluctuations was reliable. Due to the fact that all the stage drain transmitters faced identical limitations of attenuation, the seventh stage was deduced as being the source of this 24 Hz fluctuation rather than one of the other stages. This was based on the relative magnitude of the seventh stage signal shown in Figure 4 against the others. Additionally, the fourth stage was found to generate a 10 Hz pressure fluctuation that indicated the fourth stage also suffered from diffuser rotating stall. The fourth stage was left unmodified due to the lack of a substantial subsynchronous vibration component at the proximity probes for frequencies below 24 Hz.

The test crew investigated temperature measurement via the stage drains. This measurement would have allowed for an
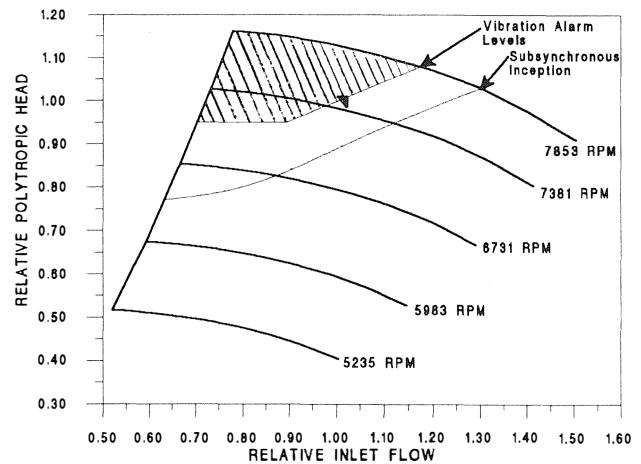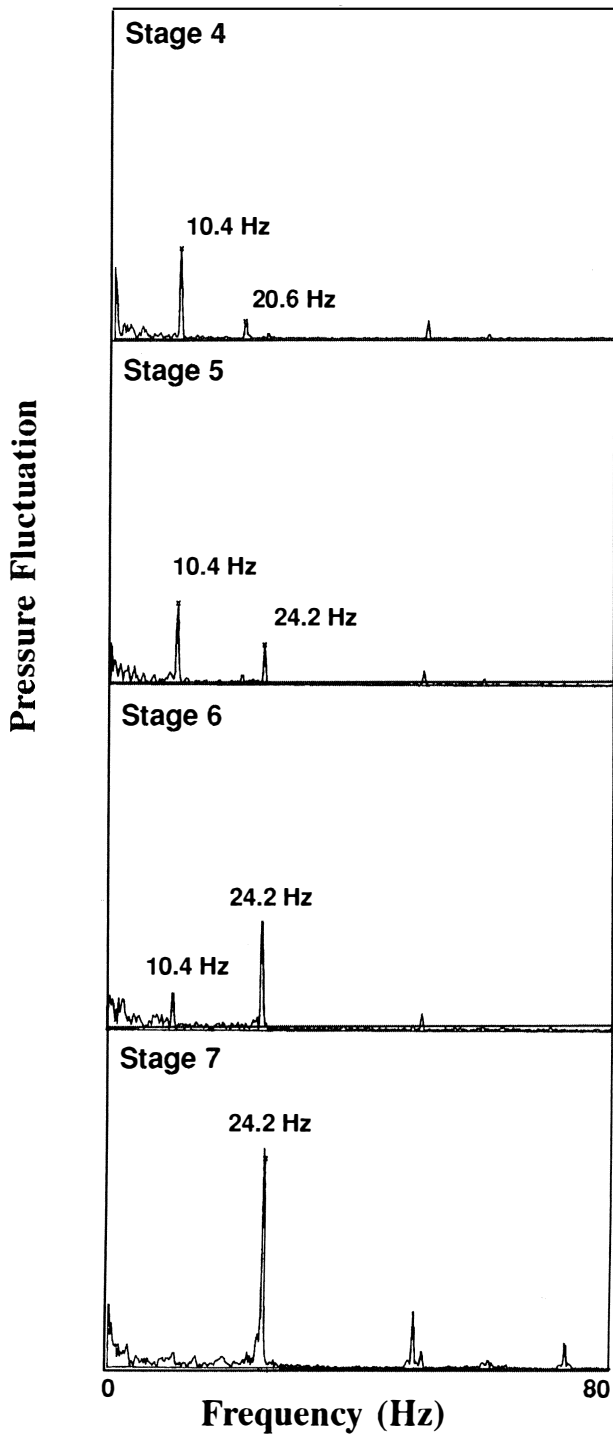
Figure 4. *Compressor Drain Pressure Spectra—Configuration II.*

Figure 5. *Compressor Vibration Spectra—Configuration III.*

concluded that no harm would come to the compressor in service. The test demonstrated the successful elimination of harmful subsynchronous vibration. Since its factory testing, the compressor has not exhibited any harmful subsynchronous vibration while operating in the field.

DIFFUSER ROTATING STALL DESIGN CRITERIA

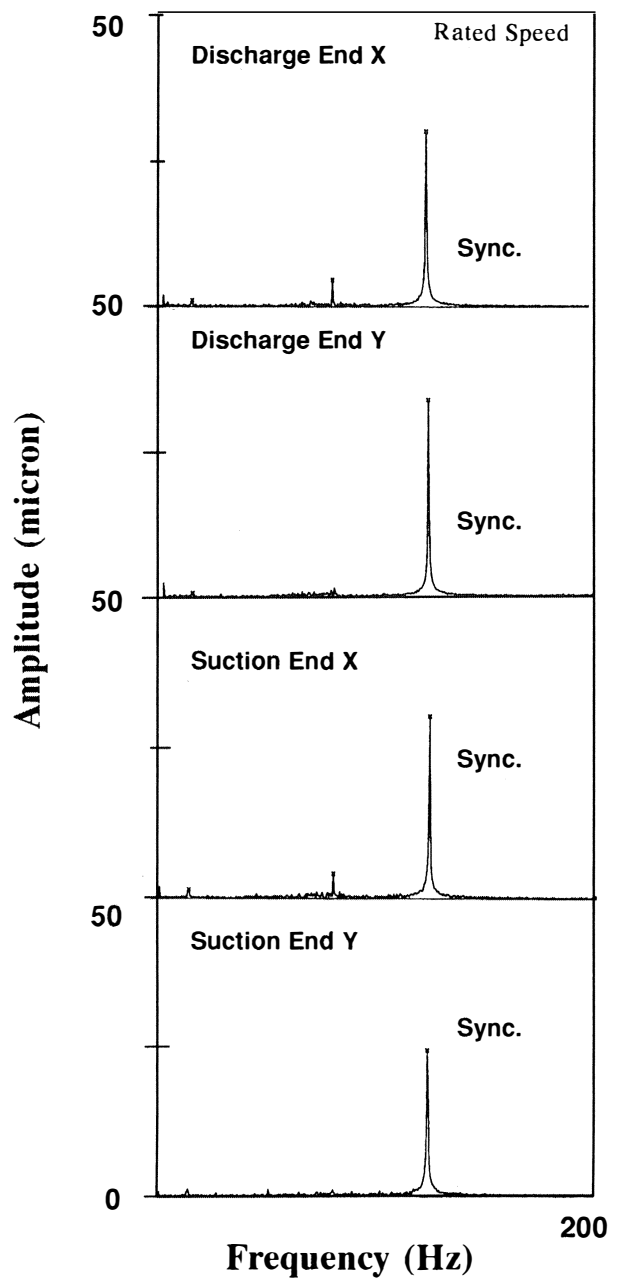The original configuration of the compressor was in compliance with the design criterion of Senoo and Kinoshita [2]. Their criterion is included in Figure 7 in the graph form of critical angle vs b_3/r_2 ratio. This criterion was based on laboratory testing by the aforementioned authors in which the tested configurations had a b_3/b_2 ratio equal to 1.0.

Final elimination of diffuser rotating stall in this high pressure compressor required large deviations from the Senoo and Kinoshita [2] criterion. The manufacturer's predicted diffuser inlet stage fluid angles (based on performance prediction at surge and rated speed) and respective margins to the Senoo and Kinoshita criterion are shown in Table 3. Regretfully, this criterion did not warn of the inception of diffuser rotating stall for either of the first two compressor configurations, despite apparent compliance. From a design perspective the extent of deviation between the actual inception of rotating stall and the Senoo and Kinoshita criterion was not acceptable. The poor correlation between the
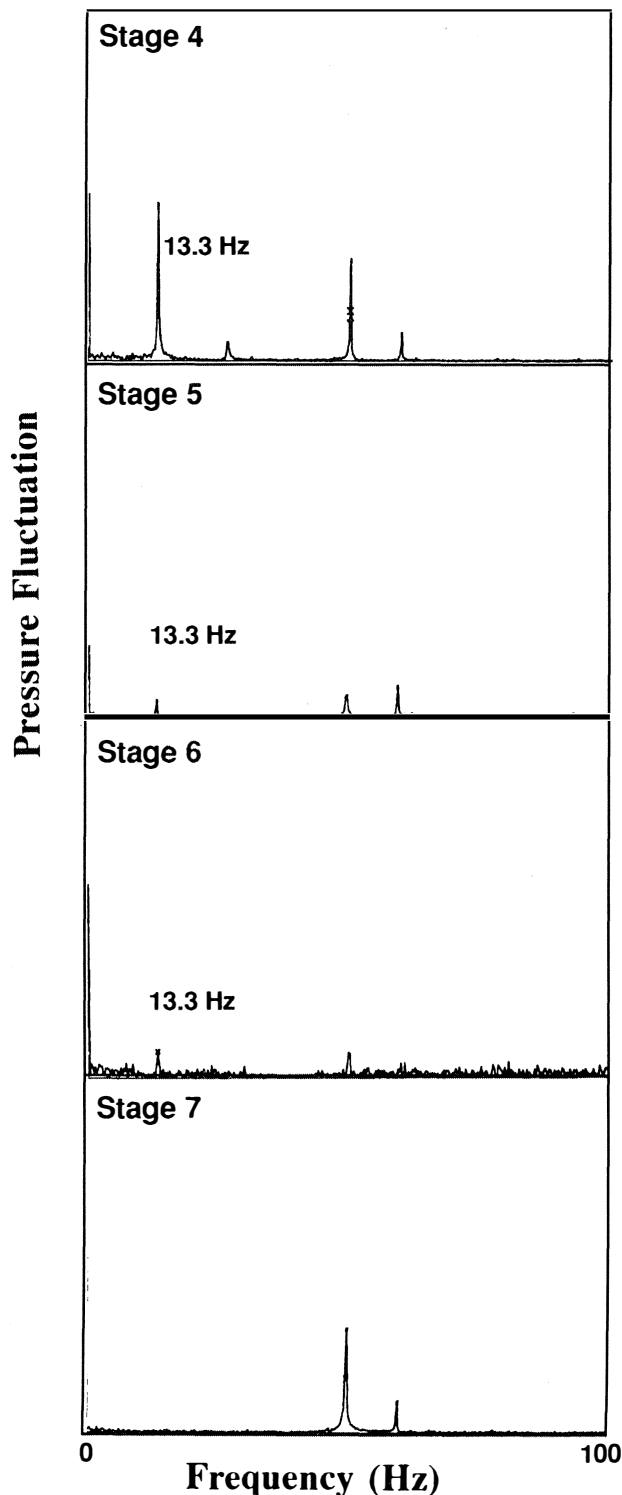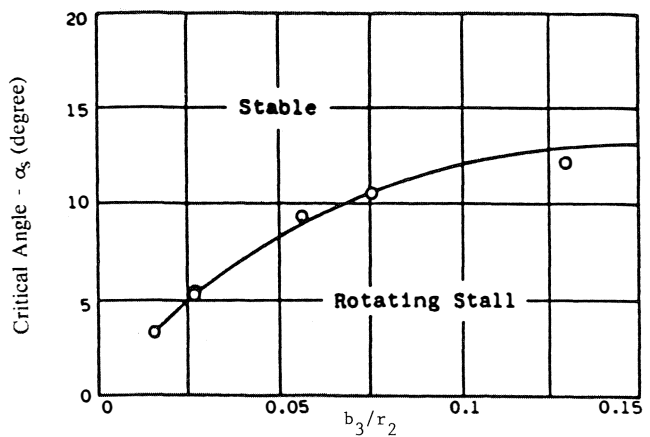
Pressure Fluctuation

Stage 4

13.3 Hz

Stage 5

13.3 Hz

Stage 6

13.3 Hz

Stage 7

0   100
Frequency (Hz)

Figure 6. Compressor Drain Pressure Spectra—Configuration III.

Ref. Senoo and Kinoshita [2] Figure 9.

Figure 7. Senoo Criterion for Vaneless Diffuser Rotating Stall.

Table 3. Inlet Diffuser Angle Prediction @ Rated Speed Surge Flow and Senoo, Et Al., Critical Angle.

Configu- ration:	I	I	III
Stage 4			
b_3/r_2	0.023	Same	Same
α_3	9.4	as	as
α_s	4.6	Cfg I	Cfg I
Stage 7			
b_3/r_2	0.028	0.024	0.016
α_3	6.0	7.3	12.2**
α_s	5.5	4.8	2.9

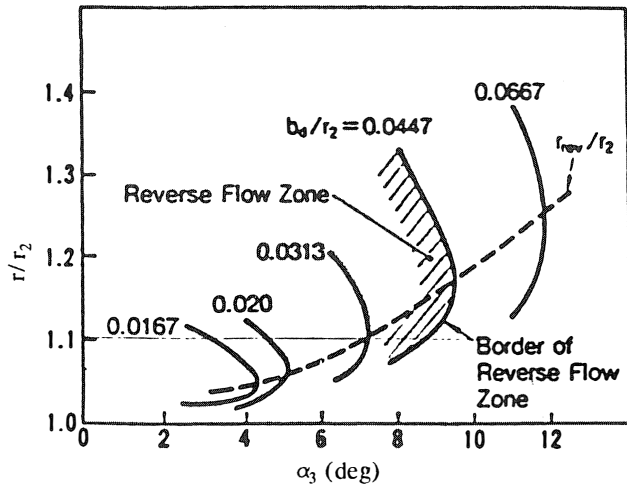* All angles are in degrees and tangentially referenced.

** Configuration III fluid angles have the additional adjustment resulting from the redirection of flow through the balance piston shunt hole, and mounting of the discharge wall to the aerodynamic bundle.

Kobayashi, et al. [3], and Nishida, et al. [4], had addressed two issues that Senoo and Kinoshita [1, 2] excluded from their work: the reductions in b_3/b_2, and the effects of diffuser inlet shape. The result of the Kobayashi, et al., work was a modification to the Senoo and Kinoshita criterion shown in Figure 8. This criterion is dependent on the Senoo and Kinoshita criteria shown in Figure 9, as it is found in Kobayashi's, et al. [3], work. An illustration of the variables used in this graph is shown in Figure 10. Proper application of the criterion required the designer to check that the diffuser inlet shape was compact in the radial direction. The design engineer could modify r_3 in order to achieve compliance.

The manufacturer's predicted diffuser inlet stage fluid angles (based on performance prediction at surge and rated speed) and respective margins to the Kobayashi, et al. [3], and Nishida, et al. [4], criterion are shown in Table 4. This criterion predicted the inception of diffuser rotating stall for both of the first two compressor configurations and the success in the third configu-

criterion and the behavior of this compressor could be explained in part by differences in the ratio of the diffuser width to impeller tip width (b_3/b_2). The use of b_3/b_2 below 1.0 was due to the industrial practice of reducing the diffuser width to avoid diffuser rotating stall. Industry has used this practice to take advantage of existing impeller designs without alteration.

$$\alpha_K = \alpha_S + (17.02 - 74.2 \times b_2/r_2) \; (1 - b_3/b_2)$$

$$\text{If } \Delta r/r_2 > 0.1 \quad \text{where } \Delta r = r_{rev} - r_3$$

Ref. Kobayashi et al. [3, 4].

Figure 8. Kobayashi, Et Al., Criterion for Vaneless Diffuser Rotating Stall.

ration. However, this apparent success must be tempered by the fact that the Kobayashi, et al., diffuser inlet shape requirement was not satisfied. Modifications in the diffuser inlet shape were not carried out and would have offered a more elegant solution; diminishing the need for the large reductions in diffuser width that were successful in eliminating the subsynchronous vibration within the operating envelope. The impact on compressor

Table 4. Inlet Diffuser Angle Prediction @ Rated Speed Surge Flow and Kobayashi, Et Al., Critical Angle.

Configuration:	I	II	III
Stage 4			
b_2/r_2	0.041	Same	Same
b_3/b_2	0.576	as	as
α_3	9.4	Cfg 1	Cfg I
α_k	11.5		
Stage 7			
b_2/r_2	0.033	0.033	0.033
b_3/b_2	0.864	0.736	0.480
α_3	6.0	7.3	12.2**
α_k	8.3	9.6	11.9

* All angles are in degrees and tangentially referenced.

** Configuration III fluid angles have the additional adjustment resulting from the redirection of flow through the balance piston shunt hole, and mounting of the discharge wall to the aerodynamic bundle.
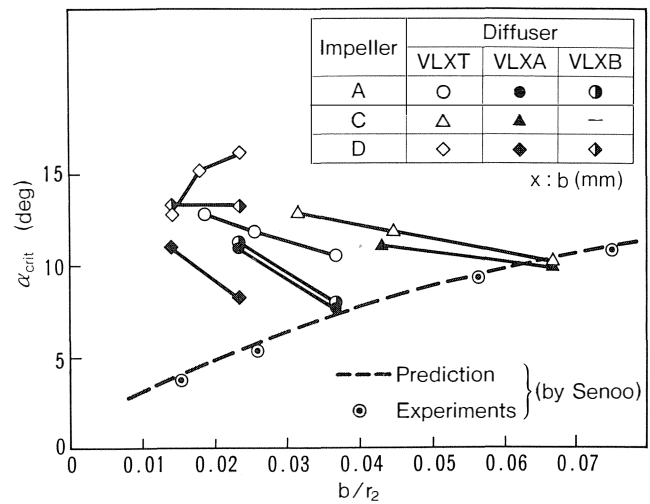
Ref. Kobayashi et al.[3] Figure 11.

Figure 9. Senoo, Et Al., Criterion for Vaneless Diffuser Rotating Stall as Published by Kobayashi, et al.

performance that resulted from the successive reductions in diffuser width would have been diminished.

DATA REDUCTION OF CONFIGURATION II

The high pressure compressor did not meet expected levels of aerodynamic performance, and the successive reductions in diffuser widths further aggravated this. The shortfall in performance accounted for a deviation in fluid angles entering the seventh stage diffuser of less than 1 degree. Due to the limited success at applying the Kobayashi, et al. [3], criterion above and the limited impact of the performance shortfall, the calculated fluid angles based on the manufactures prediction of impeller performance did not offer the confidence desired by the authors for this study. The authors initiated an effort at calculating the fluid angles based on the data of the Configuration II test.

The lack of internal temperature measurement made the direct calculation of the impeller exit angles uncertain. Therefore, the authors adopted a calculation of the exit angles using the Wiesner slip coefficient [12] as done by Senoo and Kinoshita [2]. Senoo and Kinoshita calculated the radial component based on the flowrate measured with an orifice meter. Although they did not specify how they calculated the gas density at the tip of the impeller, they had access to the tip of this isolated impeller. The multistage configuration of the tested compressor compounded the difficulty of our task, but the flange conditions and flowrates were well known from the ASME [6, 13] test measurements for all points. The data reduction combined the loop flow measurement with the measured balance seal leakage to calculate the flow and temperature at the first stage impeller eye. Pressure measurement at the individual stage drains yielded pressures at the crossovers as shown in Figure 1. The data reduction accounted for the effects of both radial equilibrium at the crossovers and the pressure rise through the vaneless diffusers in order to obtain the pressure at the exit of each impeller. To estimate the gas density at the tip of an impeller, in the absence of temperature measurements, the data reduction assumed that the compression path followed Pv^n as a constant from the first impeller to the discharge collector (the justification for this assumption is discussed later within the section on flow angle accuracy). With the given crossover pressure the data reduction calculated the tip mean radial velocity using mass flow and passage area. The data reduction used the impeller geometry, rotational speed, and the
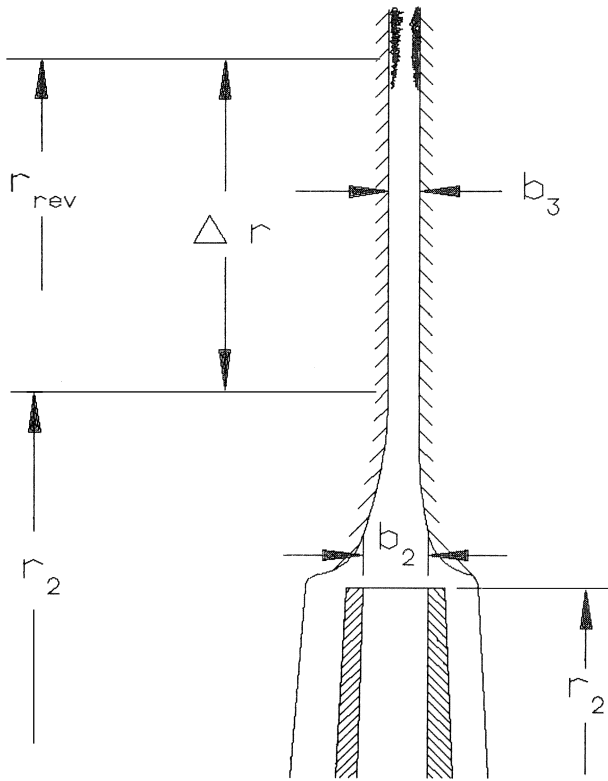
Figure 10. Diffuser Inlet Schematic

Figure 11. Seventh Stage Threshold Prediction

Wiesner slip coefficient method [12] to complete the calculation of the velocity triangle.

The authors evaluated several test points that surrounded the operating region which yielded alarm level rotor vibrations as shown in Figure 3. The last stage inlet diffuser fluid angles (α_3) for test conditions that demonstrated subsynchronous vibration, were consistently higher than the Kobayashi, et al. [3], and Nishida, et al. [4], criterion critical angle of 9.6 degrees from the tangent. The 24 Hz component of the rotor vibration at the proximity probe was present when α_3 had an approximate four degrees of margin to the Kobayashi, et al., criterion. As shown in Figure 11, the diamonds represent the test points, while the line is based on a least-mean-squares fit to the test points demonstrating the trend of the vibration amplitude. The ordinate is the gas angle margin, that is, the difference between the mean flow angle at the entrance to the parallel section of the diffuser and the criterion of Kobayashi, et al., for the inception of rotating stall. The criterion was calculated from the Kobayashi, et al., equation, reproduced here in Figure 8, and their curve for the critical flow angle when the impeller tip width and diffuser width are equal, reproduced here as Figure 9. Clearly rotating stall existed at this operating condition, well within the operating map of the compressor. The authors could not be decisive in explaining the lack of correlation offered by this data reduction, but several contributing factors offer some explanation.

The error associated with the α_3 calculation method was of concern. The triangle forming the inlet diffuser angle contained a radial and tangential component. Three sources of potential error and their effect on the radial component included:

• *Mass Flow Measurement.* An orifice meter in compliance with ASME PTC 19.5 [13] potentially yielded a 1.0 percent error amounting to a 0.1 degree variance on inlet diffuser angle. (The flow through the last stage diffuser was the net flow measured through the loop.)
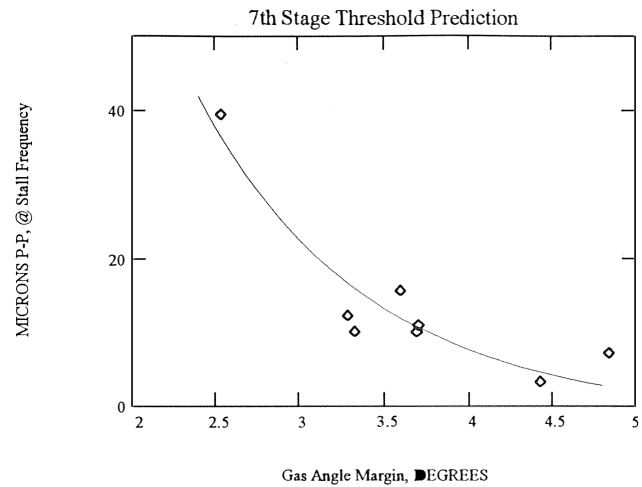
• *Passage Width.* The seventh (last) stage measurement by the capacitance proximity probe offered an accuracy of 0.005 in or 2.0 percent yielding a proportional error in the radial velocity component of the inlet diffuser angle.

• *Gas Density.* The error in the gas density at the diffuser inlet depended on several aspects of the calculation: First, the instrumentation measured, in compliance with ASME PTC 10 [6], the flange density to within 1.0 percent error. Second, the estimate of last stage diffuser pressure rise, which was approximately 2.5 percent of the total absolute pressure, was better than 1.0 percent. Third, the error introduced into the last stage calculation by assuming that Pv^n equaled a constant and that n was constant across all stages as calculated by flange measurements remains. The authors examined this last concern by a stage stacking calculation, using the expected impeller head and efficiency characteristics as a model where n was allowed to vary for each stage. Then the authors put these values into the parametric calculation. The last stage had virtually no error, since its diffuser was next to the directly measured conditions at the discharge flange.

Considering all the above errors, the estimated radial velocity component of the inlet diffuser triangle was known to five percent on the last stage.

The tangential velocity component of the inlet diffuser velocity triangle depended on the slip assumption that agrees with the assumptions of Senoo and Kinoshita [2]. Their error estimate was 2.5 percent for Wiesner's slip coefficient [12] and 2.0 degrees on impeller blade angle. Adopting these estimates and those from the radial component, the overall error in terms of α_3 was ± 0.7 degrees on the last stage.

An alternate method of calculating the tangential velocity was by stage work input. The total work input was known from the ASME PTC 10 [6] measurements. However, without individual stage temperatures, the unsatisfactory assumption of constant efficiency, as calculated from flange measurements, was required to calculate the work per stage. This method offered a calculated α_3 for the seventh stage at values ranging from 0.9 to 1.3 degrees smaller than those offered by the Wiesner slip coefficient [12] method. The larger error, associated with the assumptions of this method, led the authors not to pursue it further.

The authors examined differences in the last stage geometries between the tested compressor and the Kobayashi, et al. [3], and Nishida, et al. [4], work after determining the low level of error in their data reduction. Nishida, et al. [4], show that their

criterion is only valid when the starting radius for the reverse flow zone is 0.1 impeller radii larger than the beginning of the parallel wall section of the diffuser (Figure 10). This requirement was not met in the seventh stage in any of the configurations. Despite the lack of compliance, the subsynchronous vibration and the pressure pulsations at 24 Hz were successfully eliminated. It was achieved by forcing the fluid angle higher through successive reductions in diffuser width. As stated previously, this is not the most elegant means of removing diffuser rotating stall. The sensitivity of the diffuser inlet contour on diffuser rotating stall is still a concern. A recent publication by Sorokes [14] supports this supposition that the inlet diffuser contour had an impact on the flow behavior in this region.

CLOSURE

The aforementioned experience was an example of successfully removing a rotating stall instability. The method by which the phenomenon was removed, through successive reductions in diffuser width, has been questioned. This experience ultimately strengthens the detailed work of Kobayashi, et al. [3], and Nishida, et al. [4], and the authors agree that the Kobayashi, et al., criterion is a tool that helps to avoid diffuser rotating stall in high density multistage compressors. The Kobayashi, et al., criterion is currently the most practical and capable tool available at avoiding diffuser rotating stall instabilities. However, removing the stall is only one half of the diffuser rotating stall problem. The Configuration III testing demonstrated that aerodynamic instabilities (stage four) may be acceptable provided the gas densities are low enough. This was due to the lower level of stimulation that resulted from the reduced level of gas density or perhaps symmetry of the fourth stage stall cells. (Note the last stage was exposed to collector asymmetry.) Designing all future compressor stages to avoid diffuser rotating stall instabilities is desirable but often unnecessary. The problem with stall in this compressor was excessive shaft vibration. Others have reported dangerous blade vibrations [15]. By far, the majority of multistage industrial centrifugal compressors have been designed for relatively low density levels where they can be operated smoothly even with an aerodynamic instability such as rotating stall. To individually investigate, upgrade, and modify every compressor design is not practical and additionally threatens to reduce performance. Therefore, it is necessary to develop an analytical tool capable of quantifying the stall forces on a rotor system, using gas density, rotor speed, and other factors. Knowing these forces, the lateral vibration of a rotor system can readily be predicted by asynchronous rotor response calculations. If the response were excessive the probability of finding stall on test or in the plant could be greatly reduced by meeting the criterion of Kobayashi, et al. [3], and Nishida, et al. [4, 16].

NOMENCLATURE

b   impeller exit tip width or parallel wall radial diffuser width
N   rotational speed
n   polytropic coefficient
P   pressure
Q   volume flow
r   radius
T   temperature
v   specific volume
a   flow angle with respect to tangential or critical angle for diffuser rotating stall
r   density

SUBSCRIPTS

2   impeller exit
3   parallel wall radial diffuser inlet

d   discharge flange
i   inlet flange
K   Kobayashi, et al., critical angle
rev   beginning of reverse flow zone
S   Senoo critical angle

REFERENCES

1. Senoo, Y. and Kinoshita, Y., "Influence of Inlet Flow Conditions and Geometries of Centrifugal Vaneless Diffusers on Critical Flow Angle for Reverse Flow," ASME Journal of Fluids Engineering, pp. 98-103 (March 1977).

2. Senoo, Y. and Kinoshita, Y., "Rotating Stall Induced in Vaneless Diffusers of Very Low Specific Speed Centrifugal Blowers," ASME Journal of Engineering for Gas Turbines and Power, pp. 514-521 (April 1985).

3. Kobayashi, H., Nishida, H., Takagi, T., and Fukushima, Y., "Study on the Rotating Stall of Centrifugal Compressors," (2nd Report, Effect of Diffuser Inlet Shape on Rotating Stall), Transactions of the Japan Society of Mechanical Engineers, Part B, 56, (529), pp. 2646-2651 (in Japanese) (September 1990).

4. Nishida, H., Kobayashi, H., and Fukushima, Y., "A Study on the Rotating Stall of Centrifugal Compressors," (3rd Report, Rotating Stall Suppression Method), Transactions of the Japan Society of Mechanical Engineers, Part B, 57, (543), pp. 3794-3800 (in Japanese) (November 1991).

5. "Centrifugal Compressors for General Refinery Service," API Standard 617 Fifth Edition, American Petroleum Institute (1988).

6. "Compressor and Exhausters," ASME Power Test Code 10 (1965) (reaffirmed 1979).

7. Jansen, W., "Rotating Stall in a Radial Vaneless Diffuser," ASME Transactions, Series D: J. Basic Engineering, pp. 750-758 (December 1964).

8. Van Den Braembussche, R. A., Frigne, P., and Roustan, M., "Rotating Non Uniform Flow in Radial Compressors," AGARD CP282, Centrifugal Compressors, Flow Phenomena, Performance, pp 12-1, 12-14 (May 1980).

9. Kammer, N. and Rautenberg, M., "An Experimental Investigation of Rotating Stall Flow in a Centrifugal Compressor," ASME 82-GT-82 (1982).

10. Abdelhamid, A. N., "Control of Self-Excited Flow Oscillations in Vaneless Diffuser of Centrifugal Compressor Systems." 29, (4), Canadian Aeronautics and Space Journal, pp. 336-345 (December 1983).

11. Frigne, P. and Van Den Braembussche, R., "Distinction Between Different Types of Impeller and Diffuser Rotating Stall in a Centrifugal Compressor with Vaneless Diffusers," (106) Trans. ASME, Journal of Engineering for Gas Turbines and Power, pp. 468-474 (April 1984).

12. Wiesner, F. J., "A Review of Slip Factors for Centrifugal Impellers," ASME Journal of Engineering for Power, 89, (4), pp. 558-572 (1967).

13. "Application Part II of Fluid Meters Sixth Edition," ASME Interim Supplement 19.5 on Instruments and Apparatus (1971).

14. Sorokes, J. M., "A CFD Assessment of Entrance Area Distributions in a Centrifugal Compressor Vaneless Diffuser," ASME 94-GT-90 (1994).

15. Hasemann, U., Haupt, U., Jin, D., Seidel, U., Chen, J., and Rautenberg, M., "Rotating Stall Flow and Dangerous Blade

Excitation of Centrifugal Compressor Impeller. Part II, Case Study of Blade Failure," ASME Paper No 91-GT-103, 36th ASME International Gas Turbine and Aeroengine Congress, Orlando, Florida (1991).

16. Nishida, H., Kobayashi, H., Takagi, T., and Fukushima, Y., "A Study on the Rotating Stall of Centrifugal Compressors," (1st Report, Effect of Vaneless Diffuser Width on Rotating Stall), Transactions of the Japan Society of Mechanical Engineers, Part B, *54*, (499), pp. 589-594 (in Japanese) (March 1988).